

Reprinted from the journal

FUEL

the science and technology of Fuel and Energy

Published by Butterworth-Heinemann

FUEL

SCOPE

- petrology
- organic geochemistry
- liquefaction
- clean coal
- hydrogenation
- desulphurization
- combustion
- carbonization
- gasification
- pyrolysis
- catalysis
- fluidized-bed processes
- environmental aspects
- air pollution
- trace elements
- new materials usage

Fuel ranks among the top 5 energy and fuel science journals (from a total of 44) as quoted by the 1992 ISI Science Citation Index. This acknowledgement from independent sources reflects **Fuel's** high standards of quality – maintained for over 70 years – that include:

- Comprehensive coverage – of both traditional and emergent aspects
- A truly international spread of papers
- All papers original and refereed by experts
- Occasional Special Issues on selected symposia

A subscription to **Fuel** ensures you stay at the forefront of fuel science and technology and up-to-date with all aspects of the use, conservation, preparation, properties and reactions of a wide range of fuels including:

Asphalt * Bitumen * Coke * Coal * Graphite * Natural Gas
Oils and Gases * Oil Shale * Peat * Petroleum
Synthetic Fuels * Tar and Pitch * Tar Sands
Woods and Biomass *

PRINCIPAL EDITORS

K D Bartle University of Leeds, UK
K H van Heek DMT Institute for Cokemaking and Fuel Technology, Germany
K M Thomas University of Newcastle-Upon-Tyne, UK
J W Patrick Loughborough University, UK
F Derbyshire University of Kentucky, USA
R A Durie Turramurra, Australia

CONSULTANT

G J Lawson

CALL FOR PAPERS

By publishing your research paper in **Fuel** you will be publicizing your research around the world and in every continent. Full length papers currently have a publication time from acceptance to publication of around 10 months and letters/rapid communications take 6 months. However, to reduce this time even further, we have increased pagination in 1994.

Readers have expressed much interest in papers on environmental aspects and less usual energy sources such as solar and fuel cells – submissions in these areas are therefore particularly welcome.

No page charges are made, and the corresponding author receives 50 free off-prints and a free issue. Notes for Authors may be requested on the order form below.

INDEXING AND ABSTRACTING

Fuel is indexed/abstracted in: Current Contents; Science Citation Index; Chemical Abstracts; Energy Abstracts; Fuel and Energy Abstracts; Engineering Abstracts; Petroleum Abstracts; American Petroleum Institute (API) Abstracts; Applied Mechanics Reviews and many more.

Fuel

Volume 73 (1994) Published monthly ISSN 0016-2361
Annual subscription rates: £660.00 (Europe)
£700.00 (Rest of World)

Butterworth-Heinemann Ltd also publish two related titles, **Gas Separation & Purification** and **Fuel and Energy Abstracts** – further details are available on request.

ORDER FORM

Please send me:

- A free sample copy and subscription details of **Fuel**
- Details on advertising and reprints
- Notes for Authors
- Notes on disk submission
- Information on: **Fuel and Energy Abstracts**
 Gas Separation & Purification

Please return this form to: Catriona Burns,
Butterworth-Heinemann Ltd, Linacre House, Jordan Hill, Oxford,
OX2 8DP, UK. Tel: +44 (0) 865 310366 Fax: +44 (0) 865 310898

NAME: _____

ADDRESS _____

POSTCODE: _____ COUNTRY: _____

TELEPHONE: _____

E-MAIL: _____ FAX: _____

- 15 Goldman, J., Xie, D., Oko, A., Milne, R. and Essenhigh, R. H. in 'The Twentieth Symposium (International) on Combustion', The Combustion Institute, Pittsburgh, 1984, p. 1365
- 16 Rajan, R. R. and Wen, C. Y. *AIChE J.* 1980, **26**, 642

NOMENCLATURE

A	Cross-sectional area of the combustion chamber (m^2)
C_{air}	Total air feed rate (kmol s^{-1})
C_p	Environment oxygen concentration of a char particle (kmol m^{-3})
C_s	Oxygen concentration at external surface of a char particle (kmol m^{-3})
CO_c	CO generation due to char combustion in a combustion element (kmol s^{-1})
CO_v	Weight fraction of carbon monoxide in volatiles
$[\text{CO}]$	Concentration of carbon monoxide (kmol m^{-3})
$[\text{CO}]_c$	$[\text{CO}]$ generation due to char combustion (kmol m^{-3})
$[\text{CO}]_{\text{con}}$	$[\text{CO}]$ consumption due to combustion of carbon monoxide (kmol m^{-3})
$[\text{CO}]_v$	$[\text{CO}]$ generation due to coal devolatilization (kmol m^{-3})
$\Delta[\text{CO}]$	Change of CO concentrations through a combustion element (kmol m^{-3})
D_g	Diffusivity of oxygen ($\text{m}^2 \text{s}^{-1}$)
D_p	Diameter of a char particle (m)
\bar{D}_j	Average diameter of carbon particles in a size interval (m)
ΔD	Size interval (m)
$\Delta D_{a,j}$	Reduction of char particle size due to attrition (m)
$\Delta D_{c,j}$	Reduction of char particle size due to combustion (m)
$\Delta \bar{D}_j$	Size reduction of char particles in a size interval (m)
$f_{\text{H}_2\text{O}}$	Fraction of water in flue gas
f_{CO}	Fraction of carbon monoxide in flue gas
f_{O_2}	Fraction of oxygen in flue gas
\dot{F}_0	Feed rate of carbon (kg s^{-1})
G	Solids circulation rate ($\text{kg m}^{-2} \text{s}^{-1}$)
h	Height above primary air distribution plate (m)
h_s	Height at which secondary air is injected (m)
Δh	Thickness of a combustion element (m)
H	Total height of the combustion chamber (m)
k	Thermal conductivity of gas ($\text{W m}^{-1} \text{K}^{-1}$)
K_a	Attrition rate constant
\dot{m}_j	Inlet carbon mass flow in a size interval (kg s^{-1})
\dot{m}'_j	Outlet carbon mass flow in a size interval (kg s^{-1})
\dot{m}'_{j+1}	Outlet carbon mass flow in the nearest larger size interval (kg s^{-1})
\dot{M}	Input carbon mass flow of a combustion element (kg s^{-1})
\dot{M}_0	Initial carbon mass flow (kg s^{-1})
\dot{M}_v	Exit carbon mass flow (kg s^{-1})
$\Delta \dot{M}$	Total carbon consumption in a combustion element (kg s^{-1})
n	Number of char particle size intervals
$N(\bar{D}_j)$	Number of char particles in the size interval
N_u	Nusselt number
Δoxy	Oxygen consumption in a combustion element (kmol s^{-1})

$(\Delta \text{oxy})_c$	Oxygen consumption due to char combustion (kmol s^{-1})
$(\Delta \text{oxy})_{\text{CO}}$	Oxygen consumption due to combustion of carbon monoxide (kmol s^{-1})
$(\Delta \text{oxy})_{\text{VM}}$	Oxygen consumption due to combustion of volatiles (kmol s^{-1})
$P_j(D)$	Input char size distribution of a combustion element (m^{-1})
$P'_j(D)$	Outlet char size distribution of a combustion element (m^{-1})
$P_{c,j}(D)$	Size distribution of coal (m^{-1})
$P_{L,j}(D)$	Size distribution of char at the exit of the riser (m^{-1})
$P_{0,j}(D)$	Size distribution of char at the bottom of the riser (m^{-1})
r_D	Ratio of particle diameter to particle diameter at equilibrium conditions
R_c	Reaction rate coefficient (m s^{-1})
R_m	Mass transfer coefficient (m s^{-1})
Sc	Schmidt number
Sh	Sherwood number
t	Time (s)
Δt	Residence time of solid particles in a combustion element (s)
T_b	Gas temperature of the CFB combustor (K)
T_p	Temperature of a char particle with diameter D_p (K)
$T_{p,j}$	Temperature of a char particle with diameter \bar{D}_j (K)
U	Superficial gas velocity (m s^{-1})
U_g	Actual gas velocity (m s^{-1})
U_{mf}	Minimum fluidization velocity (m s^{-1})
U_p	Actual particle velocity (m s^{-1})
U_{sec}	Superficial gas velocity in the secondary combustion zone (m s^{-1})
X_{VM}	Proximate volatile matter content of coal (g g^{-1} coal (daf))

Greek letters

α	Secondary air-total air ratio
β	Ratio of carbon monoxide to carbon dioxide
δ	Gravimetric stoichiometric coefficient (Pa s)
ε	Voidage of a combustion cell
ε_p	Char particle emissivity
η	Total separation efficiency of a cyclone
η_c	Combustion efficiency (%)
$\eta_f(D)$	Fractional separation efficiency of a cyclone
λ	Heat of reaction (J kmol^{-1})
μ	Gas viscosity (Pa s)
ρ_c	Density of char (kg m^{-3})
ρ_g	Density of gas (kg m^{-3})
ρ_s	Density of bed solids (kg m^{-3})
ρ_t	Combustion rate of a char particle with diameter D_p based on external surface area ($\text{kmol m}^{-2} \text{s}^{-1}$)
$\rho_{t,j}$	Combustion rate of a char particle with diameter \bar{D}_j based on external surface area ($\text{kmol m}^{-2} \text{s}^{-1}$)
$\rho_{t}(\bar{D}_j)$	Combustion rate of a char particle with diameter \bar{D}_j (kmol s^{-1})
σ	Stefan-Boltzmann constant ($\text{W m}^{-2} \text{K}^{-4}$)
ϕ	Excess air ratio

3-D numerical model for predicting NO_x emissions from an industrial pulverized coal combustor

C. F. M. Coimbra, J. L. T. Azevedo and M. G. Carvalho

Instituto Superior Técnico, Mechanical Engineering Department, Av. Rovisco Pais 1096, Lisboa Codex, Portugal

(Received 18 May 1993)

The paper describes a three-dimensional computer simulation developed to predict the behaviour of industrial pulverized coal furnaces. The model was applied to a 300 MWe front-wall fired boiler under different operating conditions. The main characteristics of the current model are the use of the Lagrangian framework to describe the particulate phase, the discrete transfer model to handle the radiation transmission, and the standard $k-\epsilon$ model for turbulence treatment. The turbulent dispersion of particles is described by a new stochastic self-stable strategy. The NO_x formation mechanism is calculated in a post-processor routine. Measurements of NO_x emissions were made in the flue gases; the results agree well with those obtained by the simulations.

(Keywords: pulverized coal; combustion; NO_x emissions)

In the present decade, great improvements have been made in financial support for environmental impact studies. This may be seen as a positive response to the problem of pollution caused by the cheaper technologies. In a notable example, the modelling of pulverized coal combustors has undergone three distinct phases of methodology and purpose. The 1970s saw the transition from empirical and global approaches to local and phenomenological models¹⁻³. This kind of research and new computational power made it possible to implement more complex codes for predicting local properties of pulverized coal flames. The appearance of such numerical packages can be treated as marking a different era in the scope of coal modelling⁴⁻⁷. These models were originally developed with the aid of laboratory-scale combustor measurements and were generalized two-dimensional (axisymmetric) applications. Further union between full-scale simulations and research codes was initiated in the second half of the 1980s⁸⁻¹¹. Finally, recent environmental concerns have stimulated research on the control of pollutant emissions from industrial boilers. This is the third phase of modelling, and many studies have been made¹²⁻¹⁶.

One important feature in the development of full-scale models is the bridge between the refined numerical models intended for research-scale combustors and the models required for industrial purposes. The major limitation of computational economy imposed by the practical use of the codes does not permit many of the extravagances observed in the scientific applications. In this paper numerical strategies and realistic assumptions are described, focusing on industrial plant. NO_x emissions from a full-scale pulverized coal furnace were measured under different operating conditions and compared with predicted values. Good agreement was achieved. Both the geometry and calculation domain of the combustor

considered are sketched in *Figure 1*. The width of the furnace (x_2 -axis), not shown in the figure, was 15.0 m.

NUMERICAL MODEL

Gas phase

All local variables of interest, except the radiation ones, are calculated by solution of the generic steady-state transport equation:

$$\frac{\partial}{\partial x_i} (\rho_{;g} u_{i;g} \phi) = \frac{\partial}{\partial x_i} \left(\Gamma_{\phi}^{ef} \frac{\partial \phi}{\partial x_i} \right) + S_{\phi;g} + S_{\phi;p} \quad (1)$$

Table 1 shows the specific terms associated with each variable; note the use of the PSIC (particle-source-in-cell) model¹⁷ to account for the influence of the two phases involved. The gas-phase source terms of the three kinds of species transported (oxidant, volatiles and products) are created by the combustion model for volatiles and char oxidation. The combustion model can be addressed as an extended Magnussen and Hjertager eddy-dissipation model¹⁸, supplemented by the chemical kinetic rate of volatile combustion given by Shaw *et al.*¹⁹. The final mixing rate (R_1) is calculated by parallel competition of the two cited reaction rates²⁰:

$$R_1 = 3.5 \rho_{;g} \frac{\epsilon}{k} \min \left\{ f_{vol}, \frac{f_{O_2}}{s}, \frac{f_{CO_2}}{2(1+s)} \right\} \quad (2)$$

$$R_2 = 3.808 \times 10^5 \exp(4.8 \times 10^4 / RT_{;g}) \rho_{;g}^2 f_{vol} f_{O_2} \quad (3)$$

As a post-processor, the fuel-NO_x model is based on DeSoete's model²¹, using for the oxidation rate the suggestion given by Fiveland *et al.*¹² for industrial plant. Reduction by char and thermal NO_x generation are considered as second-order contributions and are neglected in this work.

Radiative exchange of energy is modelled by the discrete transfer model²². The code has been tested with

Table 1 Exchange terms for gas-phase transport equation (SI units)

ϕ	Γ_ϕ^{ef}	$S_{\phi;p}$	$S_{\phi;g}$
<i>Iteration loop</i>			
1	0	$\sum m_{;p}^{vol} + \sum m_{;p}^{char}$	0
u_i	$\mu_{;g}^{ef}$	$\sum M_{u_i;p}$	$\frac{\partial P}{\partial x_i} + \rho_{;g} g_i$
k	$\mu_{;g}^{ef}/0.9$	0	$\frac{\tau_{ij}}{2\mu_{;g}^t} - \rho_{;g} \varepsilon$
ε	$\mu_{;g}^{ef}/1.22$	0	$1.44 \frac{\varepsilon}{k} \frac{\tau_{ij}^2}{2\mu_{;g}^t} - 1.92 \rho_{;g} \frac{\varepsilon^2}{k}$
h	$\mu_{;g}^{ef}/0.9$	$R_t \cdot H^{vol} + S_{h;g}^{rad}$	$\sum A_{;p} n_{;p} \{h^{conv}(T_{;p} - T_{;g}) + \varepsilon_{;p} \sigma (T_{;p}^4 - T_{;g}^4)\}$
f_{O_2}	$\mu_{;g}^{ef}/0.7$	$-\sum K^{char} A_{;p} n_{;p} \frac{32}{12}$	$-R_t \cdot s \cdot f_{O_2}$
f_{vol}	$\mu_{;g}^{ef}/0.7$	$\sum K^{vol} V_{;p} n_{;p}$	$-R_t$
f_{CO_2}	$\mu_{;g}^{ef}/0.7$	$\sum K^{char} A_{;p} n_{;p} \frac{44}{12}$	$R_t \cdot s \cdot f_{CO_2}$
<i>Post-processor</i>			
f_{HCN}	$\mu_{;g}^{ef}/0.7$	0	$\frac{27}{14} S_{1;p} f_{N_2^{soal}} - w_1 - w_2$
f_{NO}	$\mu_{;g}^{ef}/0.7$	0	$w_1 - w_2$

$$w_1 = 10^{11} \rho_{;g} f_{HCN} \cdot f_{O_2^{in}} e^{-33700/T_{;g}}$$

$$w_2 = 3 \times 10^{12} \rho_{;g} f_{HCN} \cdot f_{NO} e^{-30000/T_{;g}}$$

$$\tau_{ij} = \mu_{;g}^t \left(\frac{\partial u_i}{\partial x_j} + \frac{\partial u_j}{\partial x_i} \right)$$

K^{char} = char chemical and diffusion rate

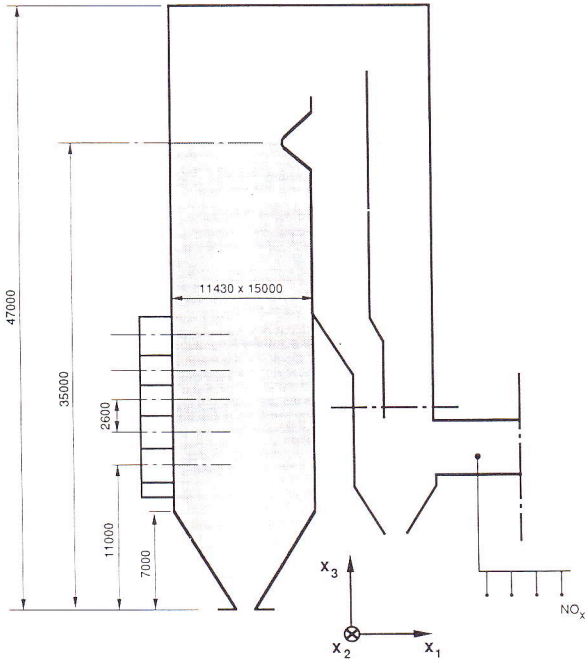
$$M_{u_i;p} = \text{particle exchange momenta} = -\frac{\partial}{\partial t} (m_{;p} u_{i;p})$$

$m_{;p}^{vol}$ = mass exchanged during devolatilization

$m_{;p}^{char}$ = mass exchanged during char combustion

K^{vol} = single devolatilization rate

$$H^{vol} = 1.015 \times 10^8 \text{ J kg}^{-1}$$


Figure 1 The combustor modelled (dimensions in mm)

different radiative properties of the gas phase. The two grey and clear gas approach by Truelove²³ was compared with combined particle and gas absorption coefficients as suggested by Boyd and Kent⁸. Since no sensible differences were obtained for the simulations presented, the latter treatment was adopted.

Particulate phase

Representative particle group behaviours are described

using the Lagrangian point of view. The equation of motion (Equation 4) is integrated by a second-order Runge–Kutta method, and the energy equation (Equation 5) is analytically solved during the particle's flight through the gas field:

$$m_{;p} \frac{\partial u_{i;p}}{\partial t} = C_D \rho_{;g} \left(\frac{A_{;p}}{2} \right) (u_{i;g} - u_{i;p}) \quad (4)$$

$$\frac{\partial}{\partial t} (m_{;p} h_{;p}) = h_{;g} \frac{\partial m_{;p}}{\partial t} + Q_{g;p}^{conv} + Q_{g;p}^{rad} + Q_{g;p}^{char} \quad (5)$$

As pointed out by many authors²⁴, the computational effort to calculate turbulent particle dispersion in large-scale pulverized coal furnaces can be very restrictive if a minimum statistical relevance is required. Quantitatively, Baxter²⁴ quotes a number between 2000 and 5000 of desirable representative trajectories to simulate monosized particles with the same starting location. Although these numbers are a function of mesh refinement, the extrapolation for predicting the particle mechanics in a full-scale combustor with 10 burners and 10 discretized values of initial particle diameter leads to the order of 10^6 different trajectories. This value is totally prohibitive from the economic standpoint.

On the other hand, the influence of turbulent particle dispersion cannot be neglected completely, because unrealistic coal flame behaviour can be obtained. The chemical species mass fractions are strongly influenced by this issue, and their distribution in space as well as the reaction locations and magnitudes requires good agreement between the real particle motion and the model handled. Research simulations of two-phase flows with high-resolution grids justify the implementation of sophisticated statistical methods such as probability density functions for propagation of position or velocity

ensembles, but this kind of approach is not compatible with many other necessary assumptions for industrial modelling (such as the use of coarse grids).

Special considerations have been invoked to link the multiple-particle technique with a stochastic dispersion model. The Boussinesq hypothesis is used to obtain the components of fluctuating velocities, and its three-dimensional correlated deviations are calculated by a conditional Gaussian distribution. The turbulence interaction is considered as acting over the minimum characteristic eddy times (eddy-cross time and eddy lifetime), as in Equation (6):

$$t^L = 0.09^{0.75} \frac{k^{1.5}}{\varepsilon} \min \left\{ \frac{1}{v_{e;p}}; \left(\frac{2k}{3} \right)^{-1/2} \right\} \quad (6)$$

For each Lagrangian-routine call, 2000 different trajectories are calculated and the random variables are averaged by an accumulative weighting expression given by²⁵:

$$\overline{S_{\phi;p}^L} = (1 - \zeta) \overline{S_{\phi;p}^{L-1}} + \zeta S_{\phi;p}^L \quad (7)$$

where

$$\zeta = L^{-1} \max \left\{ 0.5; \left(100 \sum_{i,j,k} |r_{ijk}| \right)^{-1} \right\} \quad (8)$$

and r_{ijk} is the larger value of the normalized residues (the convergence is achieved when the normalized residues remain $< 5 \times 10^{-3}$ for all generic properties). Respective weights of tracking procedure sources are then obtained in the [0.5:2] domain. Equation (8) shifts the averaged fields closely to the last iterations, in a self-stable strategy. A complete description of the Lagrangian multiple-particle technique and the turbulent particle dispersion model used in this package can be found elsewhere^{25,26}.

A specific routine of multidimensional linear transformation was created to describe the particle-wall interaction. In the toroidal section of the combustor, a single collision is modelled by one transformation Ω_k :

$$\Omega_k = (-1)^{\delta_{jk}} \{I\}, \quad j, k = 1, 2, 3 \quad (9)$$

where $\{I\}$ is the identity matrix with elements a_{ji} . In the ash-cooler zone, a specular reflection is calculated by the auxiliary matrix Ω_z :

$$\Omega_z = \begin{bmatrix} \cos 2\theta & \sin 2\theta & 0 \\ 0 & 0 & 1 \\ \sin 2\theta & -\cos 2\theta & 0 \end{bmatrix} \quad (10)$$

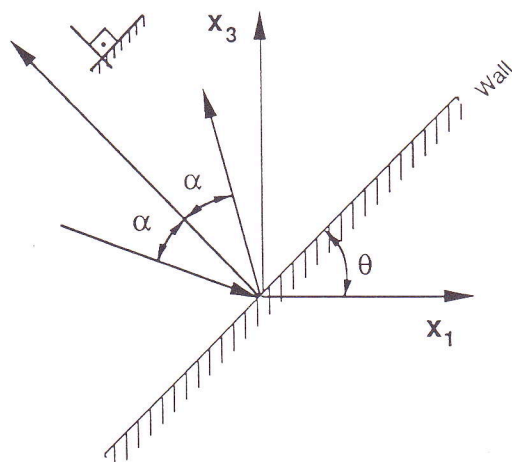


Figure 2 Collision geometry

Table 2 Analysis of coal used (wt% as-received)

Moisture	12
Volatile matter	28
Ash	10
Fixed carbon	50
Carbon	65
Hydrogen	4
Sulfur	1.1
Oxygen	6.8
Nitrogen	1.1

Table 3 Simulated operating cases

	Base case	Case 2	Case 3
Load (MW)	300	300	309
Coal (t h ⁻¹)	94	94	98
Air (t h ⁻¹)			
Primary	270	230	240
Secondary	715	720	850
BOOS (row)	–	5	1
Overfire (t h ⁻¹)	–	150	–

Figure 2 describes the impact geometry. Obviously, a multiple collision during a time step is obtained by sequential application of the linear transformations (e.g. $\Omega_1 \Omega_z \Omega_2$). This general procedure is computationally profitable and was chosen because its flexibility permits more realistic impact mechanics to be modelled. In the absence of a complete set of empirical correlations for coal-steel impacts, a totally elastic collision with no thermal energy transfer was implemented.

APPLICATION OF THE NUMERICAL CODE

The model described was applied to a full-scale industrial combustor with 20 burners assembled in four vertical rows of five burners each. Although a swirl number of 0.6 was considered as a solid rotation in the adjacent inlet velocities, a symmetric plane was assumed at the centreline of the front-wall plane. Therefore the width of calculation is reduced to half the actual dimension. This assumption is justifiable by the local importance of the swirling flow. The rotation is not perceptible far from the burners and its effects are the same, as all the rotations were made with the same orientation of angular velocity vector (which invalidates the symmetric-plane ideal). The local influence of considering a swirl number for the burners is very strong, however. Without swirl, the aspect ratio of the calculated flames is much larger than the swirling flames, altering the most important region for pollutant formation.

The analysis of the coal used is presented in Table 2. Ten different initial diameters were considered with the aid of a discretized distribution from 5 to 200 μm . The mean diameter determined by measurement was 70 μm . Table 3 summarizes the operating cases simulated by the numerical code. The base case consists of the normal operating conditions of the industrial furnace. Two different cases of BOOS (burners out of service) were simulated for full-load runs. The out-of-service row is utilized merely to provide air flow. This technique is usually used for reducing NO_x emissions, especially when the top row is used to feed overfire air.

The numerical procedure is based on a well-known volume finite discretization by staggered grids. For this paper a $22 \times 19 \times 60$ grid was implemented to simulate the half-boiler. For the discrete transfer model, a coarser grid was used ($14 \times 10 \times 27$) and 32 rays were traced from

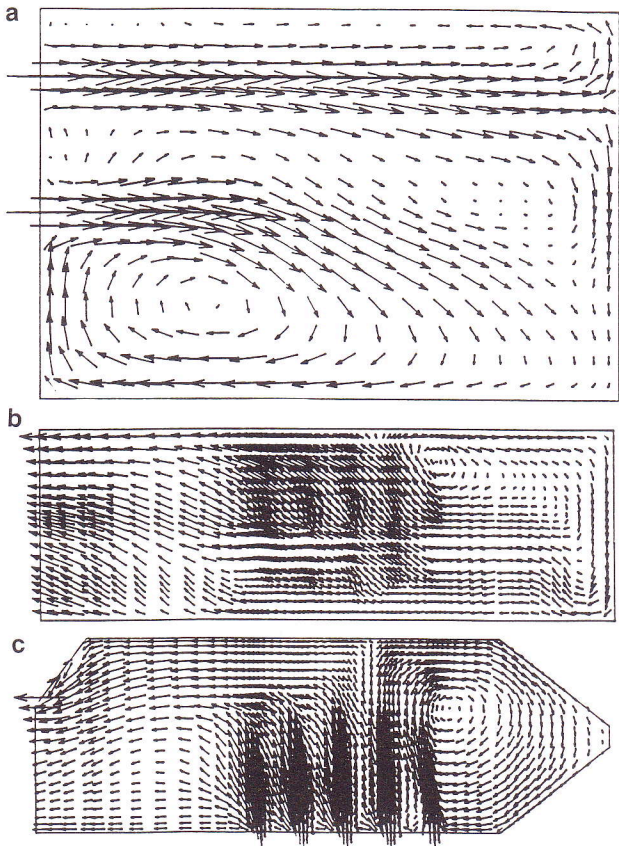


Figure 3 Predicted flow field: a, top view of plane x_1x_2 at the height of the fifth row of burners ($x_3=21.4$ m); b, front view of plane x_2x_3 ($x_1=5.4$ m); c, right-hand side view of plane x_1x_3 ($x_2=5.4$ m)

(to) each boundary superficial cell. The calculation strategy started with a partly converged solution obtained by a non-dispersive run of the Eulerian-Lagrangian code. The full-turbulence Lagrangian routine was then called every 20 iterations. The overall convergence was achieved after ~ 2000 – 2500 iterations, consuming roughly 4 h of CPU time in a VAX-9000.

RESULTS AND DISCUSSION

The presentation of the results gives prominence to the industrial situation, so the base case and case 2 are shown in more detailed fashion, whereas case 3 appears as an exercise to test the sensitivity of the model. *Figure 3* presents the predicted flow field for normal operation of the unit in three different sections of the combustor. The planes which contain burner centrelines were chosen to provide an overview of the chemical species distribution around the burners. Interestingly, the simulations show that each burner works in its own way (the operating conditions of all the burners are quite different), invalidating the separate analysis for burners (2-D axisymmetric) and for the whole furnace (3-D).

Figures 4 and *5* show the temperature distribution over the radiant section of the boiler for normal operation and case 2 respectively. *Figures 6* and *7* show the strong relation between the oxygen concentration and temperature distribution. As expected, the higher-temperature zones correspond to low oxygen concentrations. The fuel-lean regions of the combustor are characterized by oxygen mass fractions $> 5\%$. In the base case, the oxidant species is rapidly consumed by the coal combustion at all the

burners and shows a low-concentration zone above the fifth row. The highest temperatures are found just between burner levels for case 2, owing to the cold air inlet of the fifth level. For the base case, the upper zone of the combustor is a concentrated high-temperature zone. This fact is in agreement with measurements of radiant fluxes made for similar boilers under normal operating conditions and justifies the location of the intermediate superheater. In contrast, the ash-cooler zone is a hot region for case 2 (*Figure 5*), with temperatures ~ 2000 K. This can be explained by the alternative particle trajectories for this case (see *Figure 8*) and by the presence of a region of intensive combustion activity in the middle of the combustor (remember that the coal loading is the same for both cases).

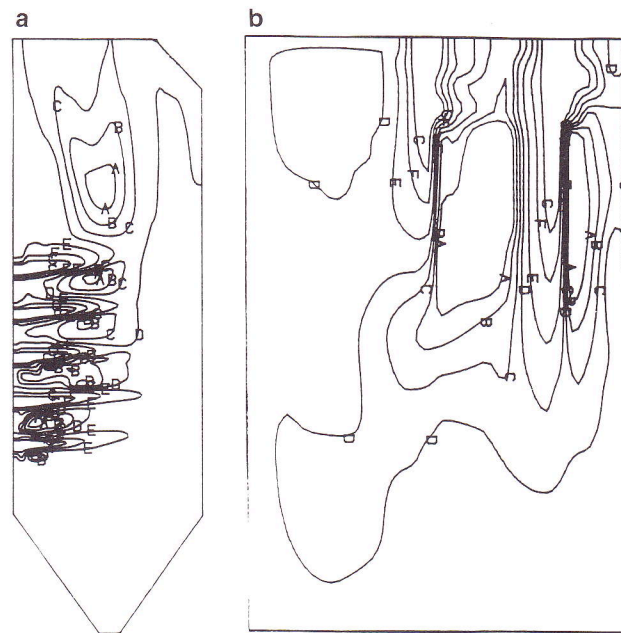


Figure 4 Predicted temperature contours for base case: a, right-hand side view of plane x_1x_3 ($x_2=5.4$ m); b, top view of plane x_1x_2 at the height of the fifth row of burners ($x_3=21.4$ m). Temperature (K): A, 2500; B, 2250; C, 2000; D, 1750; E, 1400; F, 1000; G, 700

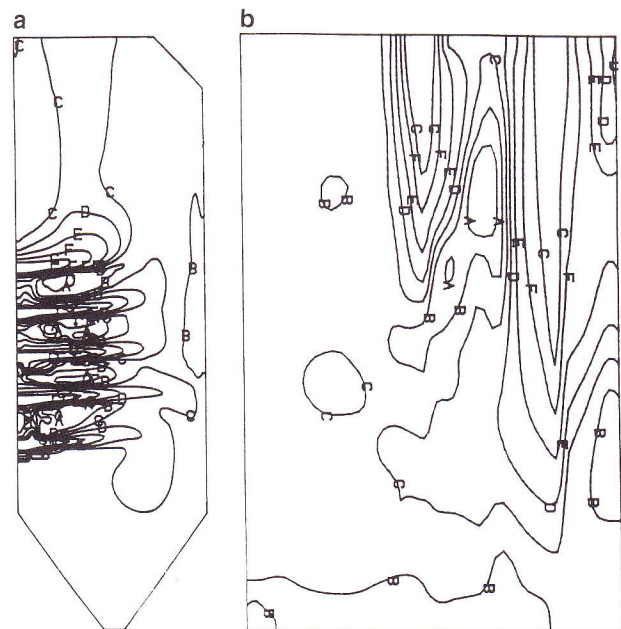


Figure 5 Predicted temperature contours for case 2: a, b and symbols as in *Figure 4*

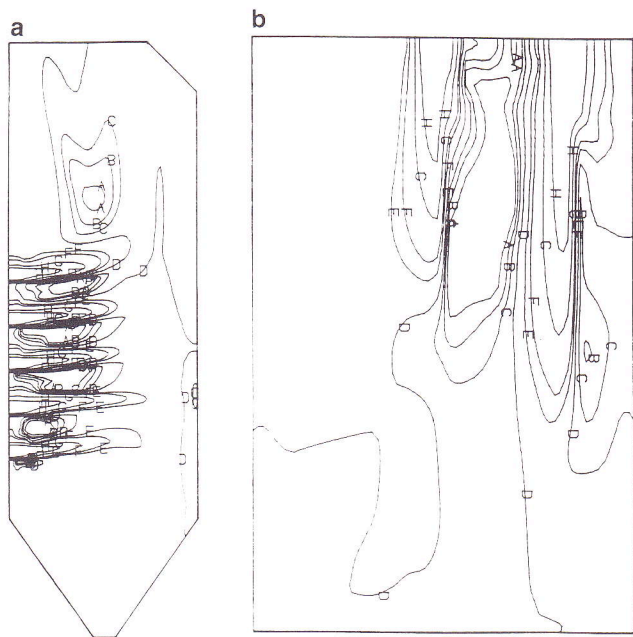


Figure 6 Predicted oxygen mass-fraction contours for base case: a, b as in Figure 4. Mass fraction (%): A, 1; B, 2; C, 3; D, 5; E, 8; F, 10; G, 15; H, 20

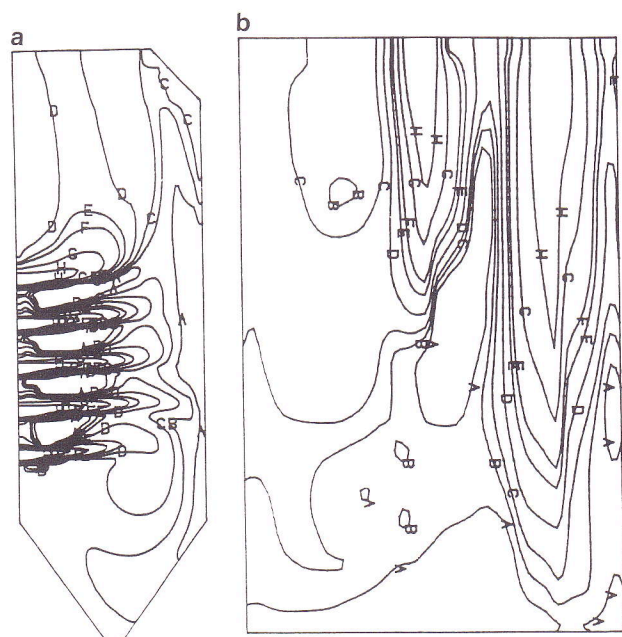


Figure 7 Predicted oxygen mass-fraction contours for case 2: a, b and symbols as in Figure 6

As all the coal volatiles are formed in the near-burner region, chemical species closely related to this process (e.g. HCN) are distributed over a fusiform convected zone coaxial with the burners. Figures 9 and 10 show the opposite phenomenon for NO generation. Since the fuel-NO formation is strongly influenced by oxygen concentration, this species is mostly formed in the envelope of the flames. In the fuel-rich regions of the flames, NO concentrations are as high as 750 ppm for case 2 and > 850 ppm for the base case. This is expected as a result of the application of DeSoete's HCN oxidation mechanism (see Table 1). For the post-processor routine used here, both char and volatiles release HCN equally, assuming a constant nitrogen concentration.

The two regions with higher NO_x concentrations shown at the top of Figure 9a are a combined result of the recirculating zones and convection from the formation area. Figure 3b shows the predicted velocity field in the central plane of the boiler parallel to the burner wall. The high velocities at the centre of this plane convect the incomplete NO formed to the low-velocity region above the fifth row of burners. The use of overfire air is successful in eliminating these transport phenomena, since the flames easily achieve the sub-stoichiometric regime, leading to lower NO_x emissions. Such a recirculating distribution as shown in Figure 9 also permits the use of reductants for pollutant species (e.g. NH₃ to combine with NO). Numerical packages such as that presented here are useful for determining optimum injection locations for such substances and their efficacy with low costs. Other than BOOS techniques, retrofitting of low-NO burners and injection of additives, there are no cheap cleanup methods for operating units.

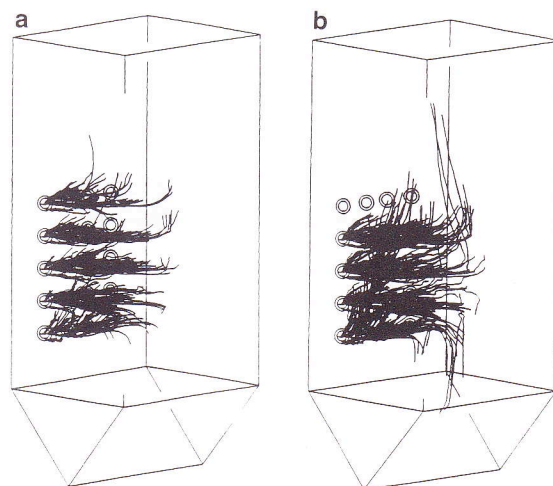


Figure 8 Representative predicted particle trajectories: a, base case; b, case 2

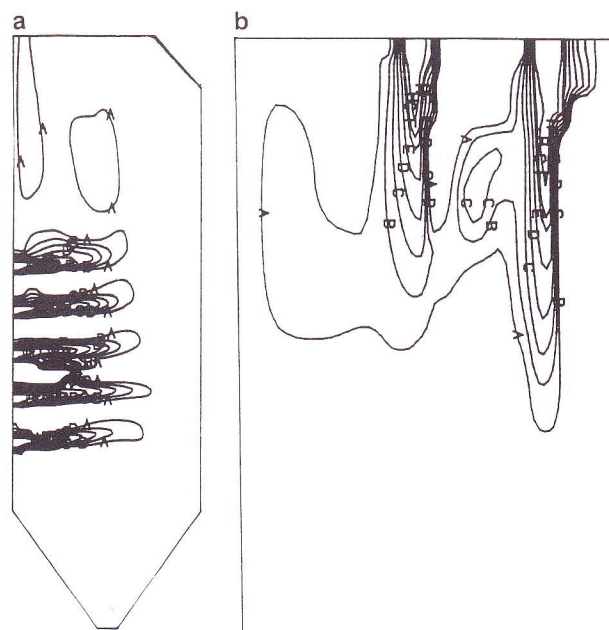


Figure 9 Predicted NO_x mass-fraction contours for base case: a, b as in Figure 4. Mass-fraction (ppmv): A, 800; B, 650; C, 500; D, 350; E, 200; F, 100; G, 70; H, 20

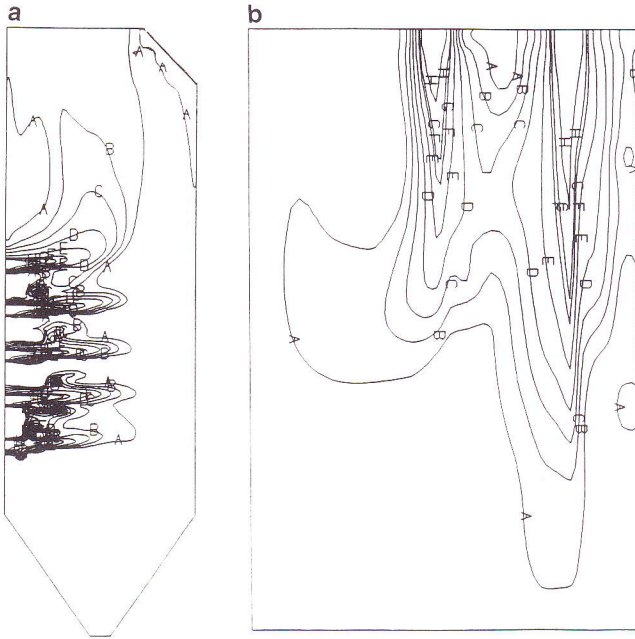


Figure 10 Predicted NO_x mass-fraction contours for case 2. a, b and symbols as in Figure 9

Table 4 Predicted and measured NO_x emissions (ppmv in flue gas)

	Base case	Case 2	Case 3
Measured	820 ± 70	780	710
Predicted	919	792	727

Table 4 compares the measured values²⁷ with the predictions for the three cases described in Table 3. Since no HCN is found at the top of the radiant section of the boiler or outside the near-burner region, NO_x concentrations at the exit of the calculation domain are considered to be equal to those measured in the flue gases. Good agreement is achieved for very different operational conditions with no tuning procedure. Despite the fact that the gas-phase combustion and the particle mechanics have been differently treated, the behaviour and response quality of the numerical code described are comparable with those of others published in the literature, corroborating the assumptions made in this work. As an example, Fiveland *et al.*¹² describes a very complete Eulerian–Eulerian code used to predict full-scale and low-NO_x cells. Temperature fluctuations were considered to influence the species distributions and a specific CO combustion mechanism was incorporated. Nevertheless, the agreement with experimental data was the same as shown here.

CONCLUSIONS

The fully three-dimensional model describing combustion, heat transfer and particle trajectories presented here provides realistic predictions of chemical species and temperature distributions, in agreement with expected values. The overall NO_x emissions are slightly over-predicted, but the sensitivity achieved is very satisfactory. The simplicity of the developed model in comparison with others may be noted. This suggests that the code can be used with some confidence for design and development calculations. The results imply that

economic Eulerian–Lagrangian approaches can be developed to describe dilute reactive two-phase flows such as that considered here.

ACKNOWLEDGEMENTS

This work was supported by the Commission of the European Communities under contract JOUF-0023-C(EDB) entitled 'The modelling of wall-fired coal burners for pollutant emission control' of the JOULE Subprogramme on Solid Fuels. Partial support from the Brazilian Scientific Agency (CAPES) to C. F. M. Coimbra is gratefully appreciated.

REFERENCES

- Gibson, M. M. and Morgan, J. A. *Int. J. Heat Mass Transfer* 1971, **14**, 141
- Lowe, A., Wall, T. F. and MacStewart, I. In 'Fifteenth Symposium (International) on Combustion', The Combustion Institute, Pittsburgh, 1975, pp. 1261–1270
- Bueters, K. A., Cogoli, J. C. and Habelt, W. W. In 'Fifteenth Symposium (International) on Combustion', The Combustion Institute, Pittsburgh, 1975, pp. 1245–1260
- Lockwood, F. C., Salooja, A. P. and Syed, S. A. *Combust. Flame* 1980, **38**, 1
- Smoot, L. C. *Prog. Energy Combust. Sci.* 1984, **10**, 229
- Truelove, J. S. In 'Twentieth Symposium (International) on Combustion', The Combustion Institute, Pittsburgh, 1984, pp. 523–530
- Rizvi, S. M. A. PhD Thesis, University of London, 1985
- Boyd, R. K. and Kent, J. H. In 'Twenty-first Symposium (International) on Combustion', The Combustion Institute, Pittsburgh, 1986, pp. 265–274
- Lockwood, F. C., Papadopoulos, C. and Abbas, A. S. *Combust. Sci. Technol.* 1988, **58**, 5
- Lee, J. J. and Lineberry, J. T. In 'International Conference on Mechanics of Two-phase Flows' (Eds S. L. Lee and F. Durst), National Taiwan University, Taipei, 1989, pp. 428–433
- Gillis, P. A. and Smith, P. J. In 'Twenty-third Symposium (International) on Combustion', The Combustion Institute, Pittsburgh, 1990, pp. 981–991
- Fiveland, W. A., Wessel, R. A. and Eskinazi, D. In 'Twenty-fourth National Heat Transfer Conference' ASME, Pittsburgh, 1987, pp. 39–49
- Smart, J. P., Knill, K. J., Visser, B. M. and Weber, R. In 'Twenty-second Symposium (International) on Combustion', The Combustion Institute, Pittsburgh, 1988, pp. 1117–1125
- Epple, B. and Schnell, U. In 'ICHMT 2nd International Forum on Expert Systems and Computer Simulation in Energy Engineering', Erlangen, FRG, 1992, CHMT, paper 121, pp. 1–12
- Kwee, H. K. In 'First International Conference on Combustion Technologies for a Clean Environment' (Eds M. G. Carvalho, F. Lockwood, W. A. Fiveland and C. Papadopoulos), Vilamoura, Portugal, 1991, pp. 16.1–16.12
- Azevedo, J. L. T. and Carvalho, M. G. In 'Fifth Workshop on Two-Phase Flows' (Ed. M. Sommerfeld), Erlangen, FRG, 1992, pp. 313–323
- Migdal, D. and Agosta, V. D. *J. Appl. Mech.* 1967, **34**(4), 860
- Magnussen, B. F. and Hjertager, B. H. In 'Sixteenth Symposium (International) on Combustion', The Combustion Institute, Pittsburgh, 1977, pp. 719–729
- Shaw, D. W., Zhu, X., Misra, M. K. and Essenhigh, R. H. In 'Twenty-third Symposium (International) on Combustion', The Combustion Institute, Pittsburgh, 1990, pp. 1152–1162
- Azevedo, J. L. T. and Carvalho, M. G. In 'First International Conference on Combustion Technologies for a Clean Environment' (Eds M. G. Carvalho, F. Lockwood, W. A. Fiveland and C. Papadopoulos), Vilamoura, Portugal, 1991, pp. 15.29–15.34
- DeSoete, G. G. In 'Fifteenth Symposium (International) on Combustion', The Combustion Institute, Pittsburgh, 1975, pp. 1093–1102
- Lockwood, F. C. and Shah, N. G. In 'Eighteenth Symposium (International) on Combustion', The Combustion Institute, Pittsburgh, 1981, pp. 1405–1414

- 23 Truelove, J. S. 'A mixed grey gas model for flame radiation', AERE Report HL76-3448-KE, 1976
- 24 Baxter, L. L. PhD Thesis, Brigham Young University, Utah, 1989
- 25 Coimbra, C. F. M. and Carvalho, M. G. In 'Fourth Brazilian Thermal Science Meeting (ENCIT)' (Eds L. P. A. Azevedo, S. L. Braza and C. W. M. Braza), Rio de Janeiro, 1992, pp. 73-76
- 26 Coimbra, C. F. M. MSc Thesis, Technical University of Lisbon, 1992
- 27 Branco, J. 'The modelling of wall fired coal burners for pollutants emission control', JOUF-0023-C(EDB), 3rd report, CEE Joule Subprogramme on Solid Fuels, 1991

u	time-averaged velocity
v_e	inlet eddy velocity
x	position coordinate
Γ	diffusion coefficient
δ_{jk}	Kronecker delta
ε	turbulent kinetic energy dissipation or emissivity
ζ	under-over adaptive relaxation factor
μ	dynamic viscosity
ρ	specific mass
σ	Stefan-Boltzmann constant
τ	stresses
ϕ	generic property
Ω	reflection matrix

NOMENCLATURE

A	superficial area
$[b]$	order of reactivity given by DeSoete ²¹
C_D	drag coefficient (a function of particle Reynolds number)
f	species mass fraction
h	enthalpy or heat transfer coefficient
K	reaction rate
k	turbulent kinetic energy
L	number of Lagrangian-routine call
M	momentum
m	mass
n	number
Q	heat
R	reaction rate for gas phase combustion model
r	normalized residues
S	source term
s	stoichiometric factor
T	temperature
t	characteristic time or simply time

Superscripts

ef	effective (turbulent + molecular)
char	related to char combustion
coal	dry ash-free basis coal
conv	convection
L	number of Lagrangian routine call
rad	radiation
t	turbulent
vol	related to the volatiles combustion

Subscripts

g	related to the gas phase
i, j, k	i, j, k direction or row index
l	line index
p	related to the particulate phase
t	total